www.czasopisma.pan.pl PAN POLSKA AKADEMIA NAUK www.journals.pan.pl

VERSITA

Arch. Min. Sci., Vol. 58 (2013), No 1, p. 165–188

Electronic version (in color) of this paper is available: http://mining.archives.pl

DOI 10.2478/amsc-2013-0012

HOSSEIN ALI LAZEMI*, MOHAMMAD FATEHI MARJI**, ALI REZA YARAHMADI BAFGHI**, KAMRAN GOSHTASBI***

ROCK FAILURE ANALYSIS OF THE BROKEN ZONE AROUND A CIRCULAR OPENING

ANALIZA PĘKNIĘCIA SKAŁY W STREFIE NARUSZONEJ WOKÓŁ OTWORU KOLISTEGO

In this paper, considering the non-linear Hoek-Brown failure criterion, a new theoretical model is presented to predict the stress components and estimate the plastic zone radius around a circular tunnel. The tunnel is excavated in an elasto-plastic rock mass subjected to plane hydrostatic and axial in situ stresses. Effects of the axial in situ stress on the plastic zone radius and stress components are studied. Based on the combination of plane hydrostatic and axial in situ stresses with the equilibrium equation and a suitable failure criterion (Hoek & Brown failure criterion), several cases are considered. For each case, the stress components, the plastic zone radius and the necessary conditions for its occurrence are determined. The results obtained by the present method are compared with those using Mohr-Coulomb criterion and with the experimental data, illustrating the validity of the present model in predicting the failure zone radius.

Keywords: Analytical solution, Hoek-Brown criterion, Plastic zone radius, axial in situ stress

W artykule zaprezentowano opracowany w oparciu o nieliniowy warunek wytrzymałości Hoeka-Browna nowy model teoretyczny przeznaczony do prognozowania składowych naprężeń i estymowania promienia strefy plastycznej wokół tunelu o przekroju kołowym. Tunel wydrążony został w sprężysto-plastycznej skale pozostającej pod wpływem płaskich stanów naprężenia (naprężeń hydrostatycznych) oraz naprężeń osiowych zarejestrowanych *in situ*. Przeanalizowano skutki oddziaływania naprężeń osiowych *in situ* na promień strefy plastycznej oraz na składowe naprężenia. Zakładając połączenie płaskich stanów naprężenia, naprężeń osiowych działających *in situ* z warunkiem równowagi i odpowiednim warunkiem wytrzymałości (warunek wytrzymałości Hoeka-Browna), przeanalizowano kilka wyodrębnionych przypadków. Dla każdego z rozważanych przypadków określono składowe naprężenia, promień

* DEPARTMENT OF MINING ENGINEERING, SCIENCE AND RESEARCH BRANCH, ISLAMIC AZAD UNIVERSITY, TEHRAN, IRAN, E-mail: hlazemi54@gmail.com (Corresponding Author)

** MINE EXPLOITATION ENGINEERING DEPARTMENT, FACULTY OF MINING AND METALLURGY, YAZD UNIVERSITY, YAZD, IRAN, E-mail: mfatehi@yazduni.ac.ir, ayarahmadi@yazduni.ac.ir

*** DEPARTMENT OF MINING ENGINEERING, FACULTY OF ENGINEERING, TARBIAT MODARES UNIVERSITY, TEHRAN, IRAN, E-mail: goshtasb@modares.ac.ir

strefy plastycznej oraz warunki niezbędne do jej wystąpienia. Wyniki uzyskane przy użyciu prezentowanej metody porównano z wynikami otrzymanymi w oparciu o warunek wytrzymałości Mohra-Coulomba oraz z danymi eksperymentalnymi, dowodząc zasadności stosowania obecnego modelu do prognozowania promienia strefy spękań.

Słowa kluczowe: rozwiązanie analityczne, kryterium wytrzymałości Mohra-Coulomba, promień strefy plastycznej, naprężenie osiowe działające *in situ*

1. Introduction

Prediction of the plastic zone radius and stress components around a circular tunnel excavated in a rock mass is an important problem in a wide variety of mining, tunneling and geotechnical engineering projects.

In the several past decades, an extensive amount of work has been done about the analysis of stresses and displacements around a circular tunnel considering various rock mass behaviors and failure criteria (Brown et al., 1983; Reed, 1986; Detournay, 1986; Wang, 1996; Lee & Pietruszczak, 2008; Carranza-Torres & Fairhurst, 1999; Carranza-Torres, 2004). Sharan presented a closed form and a simple exact solution for the stress and displacement analyses of rock mass surrounding the circular opening subjected to the hydrostatic in situ stresses (Sharan, 2003, 2005, 2008). He assumed an elastic-brittle-plastic behavior of the rock mass under plane strain condition. Park and Kim predicted the displacement around a circular opening in an elastic-brittle-plastic rock mass implementing an unassociated flow rule and validated the model with the data of the soft and hard rocks (Park & Kim, 2006). Guan et al., based on M-C failure criterion, investigated the influence of considering or not considering the unloading processing of ground on the stress distribution around tunnels (Guan et al., 2007). Wang et al. analyzed a circular tunnel in a strain softening rock mass using a numerical approach for both of M-C and H-B criteria (Wang et al., 2009). Some researches such as Salustowicz; Borecki and Chudek; and recently Chudek; Duży; Kłeczek; Majcherczyk; Tajduś and Wichur; Wichur have used the continuity of radial displacement approach to estimate the interface boundary between the elastic and plastic regions around underground openings (Salustowicz, 1965; Borecki & Chudek, 1972; Chudek, 1986; Duży, 2007; Kłeczek, 1994; Majcherczyk, 1995; Tajduś & Wichur, 2009; Wichur, 2009).

Most of the previous researches only considered the hydrostatic in situ stress conditions, but did not take into account the effect of axial in situ stress. Zhong Lu et al. presented an analytical solution for the elastic-plastic stress and plastic radius around a circular tunnel subjected to an axial in situ stress based on M-C failure criterion and showed that the plastic zone radius and stress component around a circular tunnel depend on the axial stress, P_z (Zhong Lu et al., 2010). The axial in situ stress P_z along the axis of the tunnel can not be considered arbitrary, because of the plane strain assumption. Instead, $P_z = 2\mu P$ since the axial normal strain ε_z is assumed zero. As $0 < \mu < 0.5$, P_z is always less than P. In fact, the horizontal in situ stresses are sensitive to the direction. The difference between the maximum and minimum horizontal stress at the same depth can be large, and depends on the local geological condition (Zhong Lu et al., 2010).

On the other hand, it is obvious that the considered failure criterion in the simulation of the rock behavior plays an important role. In this paper, implementing the non-linear failure criterion (Hoek-Brown), the plastic zone radius and stress component around a circular tunnel subjected to a plane hydrostatic and an axial in situ stresses are determined. The results are compared with

those of linear failure criterion (Mohr-coulomb) and with the experimental data available in the literature (*Technical Deputy*..., 2002). This comparison demonstrates the validity of the proposed method and illustrates the accuracy of the results obtained by using the present model.

2. Elastic and plastic zones around a circular tunnel

Based on the theory of plasticity, the radial stress, σ_r, and the tangential stress, σ_θ, in the rock mass around a circular tunnel subjected to the plane hydrostatic in situ stress, P, and the axial stress P_z, depend only on the value of P but not on the value of P_z. Furthermore, the axial stress component, σ_z, is equal to P_z and does not relates to r (Fig. 1). The elastic and plastic zones around the tunnel are considered to be continuous and it is assumed that there is continuity between the elastic and plastic stresses for the interface between them (at the interface the elastic and plastic stresses are equal) (Guan et al., 2007). It should be noted that in this paper, the concept of axial stress P_z is the same as that given in reference (Zhong Lu et al., 2010).

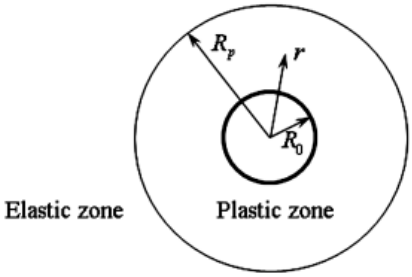

Fig. 1. Circular tunnel with its components

In the quasi-plane strain problems, the radial stress, σ_r, is the minor principal stress, whether the major principal stress can be considered as the tangential stress, σ_θ, or the axial stress, σ_z. Assuming the various values of P and P_z (which will be discussed in section 4), several different cases can be considered in the plastic zone:

Case 1: $\sigma_\theta > \sigma_z$, for all points around the tunnel (Fig. 2-a).

Case 2: $\sigma_\theta = \sigma_z$ for $R_0 \le r \le R_1$, and $\sigma_\theta > \sigma_z$ for $R_1 \le r \le R_p$, in which R_0 is the radius of tunnel and R_1 and R_p are the radii of plastic zone (Fig. 2-b).

Case 3: $\sigma_\theta = \sigma_z$, for all points around the tunnel (Fig. 2-c).

Case 4: $\sigma_\theta = \sigma_z$ for $R_0 \le r \le R_1$, and $\sigma_z > \sigma_\theta$ for $R_1 \le r \le R_p$ (Fig. 2-d).

Case 5: $\sigma_z > \sigma_\theta$, in all points around the tunnel (Fig. 2-e).

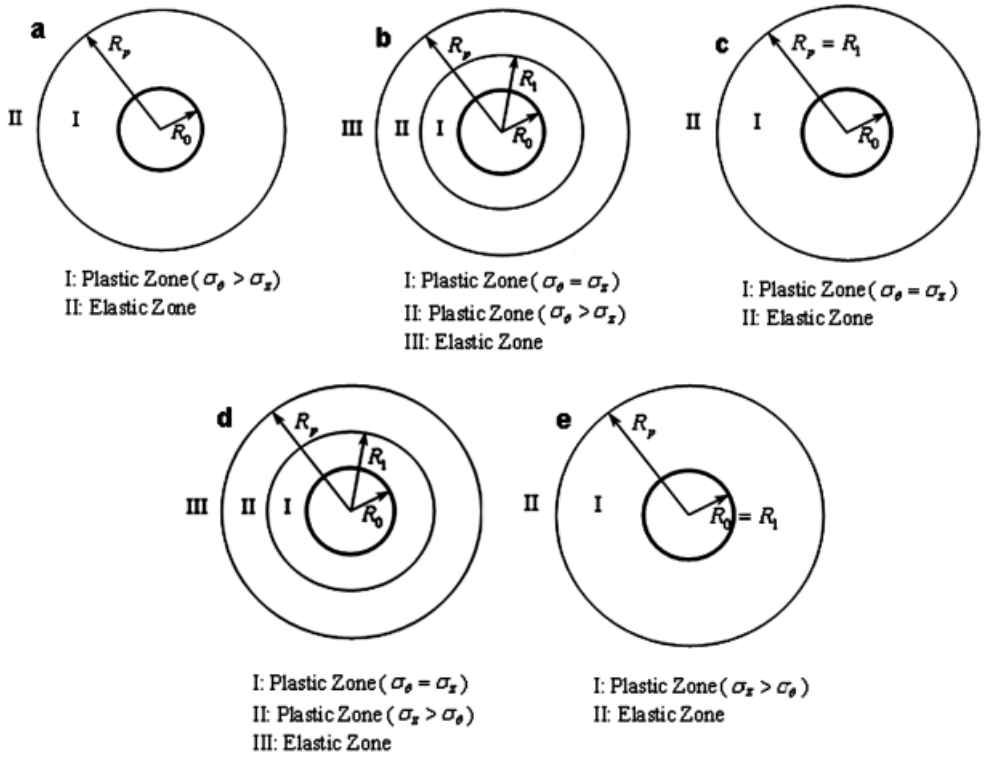

Fig. 2. Different failure zones around a circular tunnel

3. Failure Analysis

3.1. Case 1

The equilibrium equation in polar coordinates (Brady & Brown, 2004) can be written as:

$$\frac{d\sigma_r}{dr} + \frac{\sigma_r - \sigma_\theta}{r} = 0 \tag{1}$$

On the other hand, the Hoek-Brown failure criterion is (Hoek & Brown, 1980):

$$\sigma_1 = \sigma_3 + \left(m\sigma_3\sigma_c + s\sigma_c^{\,2}\right)^{\frac{1}{2}} \tag{2}$$

where σ_1 is the major principal stress at failure, σ_3 is the minor principal stress at failure, σ_c is the uni-axial compressive strength of the intact rock material, m and s are the material constants which depend on the properties of the rock and on the extent to which it has been broken before being subject to the stresses ($s = 1$ for intact rock and $s < 1$ for previously broken rock).

It was mentioned that for the quasi-plane strain problems, σ_r, is always the miner principal stress, so $\sigma_3 = \sigma_r$. In addition in cases 1, 2, and 3 $\sigma_\theta \geq \sigma_z$, so $\sigma_1 = \sigma_\theta$, while in cases 4 and 5, $\sigma_z \geq \sigma_\theta$ and $\sigma_1 = \sigma_z$.

Rewriting the Hoek-Brown failure criterion for case 1 (Fig. 2-a) results in:

$$\sigma_\theta = \sigma_r + \left(m\sigma_r\sigma_c + s\sigma_c^2\right)^{\frac{1}{2}} \tag{3}$$

Substituting Eq. (3) into Eq. (1) gives

$$\frac{d\sigma_r}{dr} - \frac{1}{r}\left(m\sigma_r\sigma_c + s\sigma_c^2\right)^{\frac{1}{2}} = 0 \tag{4}$$

This equation can be solved using the separation of variables method (Keryszig, 2006). Rearranging Eq. (4) leads to the following differential equation

$$\frac{d\sigma_r}{\left(m\sigma_r\sigma_c + s\sigma_c^2\right)^{\frac{1}{2}}} = \frac{dr}{r} \tag{5}$$

Integrating the two sides of Eq. (5) results in:

$$\frac{2}{m\sigma_c}\left[\left(m\sigma_r\sigma_c + s\sigma_c^2\right)^{\frac{1}{2}}\right] = Ln\,r + C_1 \tag{6}$$

where C_1 is a constant parameter and can be determined from the boundary condition in R_0, where $\sigma_r = 0$, therefore,

$$C_1 = \frac{2s^{\frac{1}{2}}}{m} - Ln\,R_o \tag{7}$$

σ_r can be simplified in the following form in which the constants of C_1, C_2 and C_3 are defined in Eqs. (7), (9), and (10) respectively.

$$\sigma_r = C_3(Ln\,r + C_1)^2 + C_2 \tag{8}$$

$$C_2 = -\frac{S\sigma_c}{m} \tag{9}$$

$$C_3 = \frac{m\sigma_c}{4} \tag{10}$$

Substituting Eq. (8) into Eq. (3) gives

$$\sigma_\theta = C_3(Ln\,r + C_1)^2 + 2C_3(Ln\,r + C_1) + C_2 \tag{11}$$

The axial stress σ_z can be determined by using the stress-strain relationship (generalized Hook's law (Popov, 1990)) as

$$\sigma_z = \mu(\sigma_\theta + \sigma_r) + P_z - 2\mu P \tag{12}$$

where μ is the Poisson's ratio. Substituting Eqs. (8) and (11) into Eq. (12) leads to

$$\sigma_z = 2\mu\left[C_3(Ln\,r + C_1)^2 + C_3(Ln\,r + C_1) + C_2\right] + P_z - 2\,\mu P \tag{13}$$

The stresses in the elastic zone ($R_p \le r \le \infty$) can be given directly by the theory of elasticity (Popov, 1990; Timoshenko, 2010; Saad, 2009) as

$$\sigma_r = P - \frac{C_4^I}{r^2} \tag{14}$$

$$\sigma_\theta = P + \frac{C_4^I}{r^2} \tag{15}$$

$$\sigma_z = P_z \tag{16}$$

The constant parameter, C_4^I in Eqs. (14) and (15) and the plastic zone radius, R_p, can be obtained using the continuity condition of stresses at the elastic-plastic interface ($r = R_p$) as:

$$at\ r = R_p\ , \qquad \sigma_r|_{Plastic} = \sigma_r|_{Elastic} \tag{17-a}$$

$$at\ r = R_p\ , \qquad \sigma_\theta|_{Plastic} = \sigma_\theta|_{Elastic} \tag{17-b}$$

Substituting Eqs. (8) and (11) as the plastic stress components and Eqs. (14) and (15) as the elastic stress components in Eq. (17) gives

$$C_3(Ln\,R_p + C_1)^2 + C_2 = P - C_4^I / R_p^2 \tag{18}$$

$$C_3(Ln\,R_p + C_1)^2 + 2C_3(Ln\,R_p + C_1) + C_2 = P + C_4^I / R_p^2 \tag{19}$$

Solving Eqs. (18) and (19) simultaneously for the unknowns R_p and C_4^I (see Appendix A) gives

$$R_p = \exp\left[-\frac{1}{2} + \sqrt{\frac{1}{4} + \frac{P - C_2}{C_3}} - C_1\right] \tag{20}$$

$$C_4^I = R_p^2\left[P - C_3(Ln\,R_p + C_1)^2 + C_2\right] \tag{21}$$

3.2. Case 2

As shown in Fig. 2-b, in the plastic zone I ($R_0 \le r \le R_1$), $\sigma_\theta = \sigma_z$, while in the plastic zone II ($R_1 \le r \le R_p$), $\sigma_\theta > \sigma_z$. The results for the radial and tangential stress components, σ_r and σ_θ, in plastic zones I and II, are almost the same as given in Eqs. (8) and (11), respectively. In addition, the axial stress component, σ_z, in the plastic zone I is equal to σ_θ and in the plastic zone II can be determined from Eq. (13). The stress component in the elastic zone III, are similar as given in Eqs. (14) to (16). It should be noted that the constant C_4^I should be replaced with the new unknown constant C_4^{II}.

Using the continuity condition of stresses at the interface between zones I and II ($r = R_1$) and at the interface between zones II and III ($r = R_p$), the radius R_1 of the plastic zone I, the radius R_p of the plastic zone II, and the unknown constant C_4^{II} can be calculated.

The continuity condition of σ_z between the plastic zones I and II should be established as:

$$at\ r = R_1\ , \qquad \sigma_z|_{Zone\ I} = \sigma_z|_{Zone\ II} \tag{22}$$

In the plastic zone I, σ_z is equal to σ_θ (which is given by Eq. (11)). In the plastic zone II, σ_z can be calculated from Eq. (13). Replacing r in Eqs. (11) and (13) with R_1 and substituting them into Eq. (22) leads to:

$$\begin{aligned} &C_3(LnR_1 + C_1)^2 + 2C_3(LnR_1 + C_1) + C_2 = \\ &\qquad = 2\mu[C_3(LnR_1 + C_1)^2 + C_3(LnR_1 + C_1) + C_2] + P_z - 2\mu P \end{aligned} \tag{23}$$

Solving Eq. (23) for R_1, (see Appendix B) gives

$$R_1 = \exp\left[\frac{-m_2 - \left(m_2^2 - 4m_1m_3\right)^{\frac{1}{2}}}{2m_1} - C_1\right] \tag{24}$$

where

$$m_1 = 2C_3\mu - C_3 \tag{25}$$

$$m_2 = 2C_3\mu - 2C_3 \tag{26}$$

$$m_3 = 2C_2\mu + P_z - 2\mu P - C_2 \tag{27}$$

The continuity condition for σ_r and σ_θ between the plastic zones II and III should be established as

$$at\ r = R_p\ , \qquad \sigma_r|_{Zone\ II} = \sigma_r|_{Elastic} \tag{28-a}$$

$$at\ r = R_p\ , \qquad \sigma_\theta|_{Zone\ II} = \sigma_\theta|_{Elastic} \tag{28-b}$$

Since the stress components for the plastic zone II and the elastic zone are similar to those of case 1, the equations for R_p and C_4^{II} will be the same too i.e.

$$R_p = \exp\left[-\frac{1}{2} + \sqrt{\frac{1}{4} + \frac{P - C_2}{C_3}} - C_1\right] \tag{29}$$

$$C_4^{II} = R_p^2[P - C_3(Ln\,R_p + C_1)^2 + C_2] \tag{30}$$

3.3. Case 3

Fig. 1-b and Fig. 1-c illustrate that case 3 is the same as case 2, where $R_1 = R_p$. Therefore, in case 3, σ_r and σ_θ for the plastic zone can be determined from Eqs. (8) and (11), respectively. On the other hand, σ_z is equal to σ_θ which can be obtained from Eq. (11). It is obvious that the elastic stress components and the plastic zone radius, R_p, are the same as those of case 2.

3.4. Case 4

For case 4, the plastic zone I ($R_0 \le r \le R_1$), σ_θ is equal to σ_z, so both of them can be considered as the major principal stress. In other words, the failure criterion can be rewritten as Eq. (3). Therefore, in zone I, the stresses can be obtained as explained in section 3.1 and are the same as those given by Eqs. (8) and (11).

In the plastic zone II ($R_1 \le r \le R_p$), σ_z is greater than σ_θ, so σ_z is the major principal stress and the H-B failure criterion will be changed to the following equation

$$\sigma_z = \sigma_r + \left(m\sigma_r\sigma_c + s\sigma_c^2\right)^{\frac{1}{2}} \tag{31}$$

It should be noted that the equilibrium equation is still Eq. (1). The radial, tangential and axial plastic strain components can be obtained from the following equation by replacing the subscript i with r, θ and z, respectively (Zhong Lu et al., 2010).

$$d\varepsilon_i^p = \frac{\partial f}{\partial \sigma_i} d\lambda \tag{32}$$

where λ is the proportional coefficient and f is the associated flow rule which can be written as

$$f = \sigma_z - \left[\sigma_r + \left(m\sigma_r\sigma_c + s\sigma_c^2\right)^{\frac{1}{2}}\right] \tag{33}$$

Substituting Eq. (33) into Eq. (32) results in:

$$d\varepsilon_r^p = \frac{\partial f}{\partial \sigma_r} d\lambda = \left[-1 - \frac{1}{2}\; m\sigma_c\left(m\sigma_r\sigma_c + s\sigma_c^2\right)^{-\frac{1}{2}}\right] d\lambda \tag{34}$$

$$d\varepsilon_\theta^p = \frac{\partial f}{\partial \sigma_\theta} d\lambda = 0 \tag{35}$$

$$d\varepsilon_z^p = \frac{\partial f}{\partial \sigma_z} d\lambda = d\lambda \tag{36}$$

The plastic strain can be obtained (by integrating Eqs. (34), (35) and (36)) as

$$\varepsilon_r^p = \left[-1 - \frac{1}{2} \; m\sigma_c \left(m\sigma_r \sigma_c + s\sigma_c^2 \right)^{-\frac{1}{2}} \right] \lambda \tag{37}$$

$$\varepsilon_\theta^p = 0 \tag{38}$$

$$\varepsilon_z^p = \lambda \tag{39}$$

The total strain equals to the sum of the elastic and plastic strain components, which can be derived as

$$\varepsilon_r = \varepsilon_r^e + \varepsilon_r^p = \varepsilon_r^e - \left[-1 + \frac{1}{2} \; m\sigma_c \left(m\sigma_r \sigma_c + s\sigma_c^2 \right)^{-\frac{1}{2}} \right] \lambda \tag{40}$$

$$\varepsilon_\theta = \varepsilon_\theta^e + \varepsilon_\theta^p \tag{41}$$

$$\varepsilon_z = \varepsilon_z^e + \varepsilon_z^p = \varepsilon_z^e + \lambda = \varepsilon_0 \tag{42}$$

in which ε_0 is a non-zero constant in a quasi-plane strain problem and is equal to $(P_z - 2\mu P)/E$ (E is young modulus of the rock mass).

The elastic strain components can be determined from Hook's law as:

$$\varepsilon_r^e = \frac{1}{E} \left[\sigma_r - \mu(\sigma_\theta + \sigma_z) \right] \tag{43}$$

$$\varepsilon_\theta^e = \frac{1}{E} \left[\sigma_\theta - \mu(\sigma_r + \sigma_z) \right] \tag{44}$$

$$\varepsilon_z^e = \frac{1}{E} \left[\sigma_z - \mu(\sigma_r + \sigma_\theta) \right] \tag{45}$$

Solving Eq. (42) for λ results in:

$$\lambda = \varepsilon_0 - \varepsilon_z^e \tag{46}$$

The compatibility equation of strains is (Timoshenko, 2010):

$$\frac{d\varepsilon_\theta}{dr} = \frac{\varepsilon_r - \varepsilon_\theta}{r} \tag{47}$$

Substituting Eqs. (40), (41), (42) and (46) into Eq. (47) lead to

$$\frac{d\varepsilon_\theta^e}{dr}=\frac{1}{r}\left\{\varepsilon_r^e-\left[1+\frac{1}{2}m\sigma_c(m\sigma_r\sigma_c+s\sigma_c^{\,2})^{-\frac{1}{2}}\right](\varepsilon_0-\varepsilon_z^e)-\varepsilon_\theta^e\right\} \tag{48}$$

Derivation of Eq. (44) with respect to r gives

$$\frac{d\varepsilon_\theta^e}{dr}=\frac{1}{E}\frac{d\sigma_\theta}{dr}-\frac{\mu}{E}\left(\frac{d\sigma_r}{dr}+\frac{d\sigma_z}{dr}\right) \tag{49}$$

Substituting Eqs. (43), (44), (45) and (49) into Eq. (48) lead to

$$\begin{aligned}\frac{d\sigma_\theta}{dr}-\mu\left(\frac{d\sigma_r}{dr}+\frac{d\sigma_z}{dr}\right)=\frac{1}{r}\Big\{&\left[\sigma_r-\mu(\sigma_\theta+\sigma_z)\right]-\left[1+\frac{1}{2}m\sigma_c(m\sigma_r\sigma_c+s\sigma_c^{\,2})^{-\frac{1}{2}}\right]\\&\left[E\varepsilon_0-\sigma_z+\mu(\sigma_r+\sigma_\theta)\right]-\left[\sigma_\theta-\mu(\sigma_r+\sigma_z)\right]\Big\}\end{aligned} \tag{50}$$

Derivation of Eq. (31) with respect to r gives

$$\frac{d\sigma_z}{dr}=\left[1+\frac{1}{2}m\sigma_c\left(m\sigma_r\sigma_c+s\sigma_c^{\,2}\right)^{-\frac{1}{2}}\right]\frac{d\sigma_r}{dr} \tag{51}$$

In addition, solving Eq. (1) for σ_θ results in:

$$\sigma_\theta=\sigma_r+r\frac{d\sigma_r}{dr} \tag{52}$$

Derivation of Eq. (52) with respect to r gives

$$\frac{d\sigma_\theta}{dr}=2\frac{d\sigma_r}{dr}+r\frac{d^2\sigma_r}{dr^2} \tag{53}$$

Substituting Eqs. (31), (51), (52) and (53) into Eq. (50) lead to a second order differential equation for σ_r as

$$r^2\frac{d^2\sigma_r}{dr^2}+3r\frac{d\sigma_r}{dr}=g(\sigma_r) \tag{54}$$

where $g(\sigma_r)$ is defined as:

$$\begin{aligned}g(\sigma_r)=\sigma_r&\left[1+\frac{1}{2}m\sigma_c\left(m\sigma_r\sigma_c+s\sigma_c^{\,2}\right)^{-\frac{1}{2}}\right](1-2\mu)+\left(m\sigma_r\sigma_c+s\sigma_c^{\,2}\right)^{\frac{1}{2}}\\&-E\varepsilon_0-\frac{1}{2}E\varepsilon_0 m\sigma_c\left(m\sigma_r\sigma_c+s\sigma_c^{\,2}\right)^{-\frac{1}{2}}+\frac{1}{2}m\sigma_c\end{aligned} \tag{55}$$

The radial stress, σ_r, can be determined by solving Eq. (54). Finally, the tangential and axial stress components, σ_θ and σ_z, can be obtained by substituting σ_r into Eq. (52) and Eq. (31), respectively. Eq. (54) is a second order differential equation, so requires two boundary conditions for its solution. Furthermore, the plastic zone radii, R_1 and R_p are the two additional unknown parameters.

The stress components in the elastic zone III, are similar to those given by Eqs. (14)-(16). It should be noted that the constant C_4^I should be replaced with the new unknown constant C_4^{IV}. In order to determine the five unknown parameters, R_1, R_p, C_4^{IV} and the two constant parameters (results from the solution of the differential equation given by Eq. (54)), five boundary conditions are required. These boundary conditions can be obtained from

$$at\ r = R_1\ , \qquad \sigma_r|_{Zone\ I} = \sigma_r|_{Zone\ II} \tag{56-a}$$

$$at\ r = R_1\ , \qquad \sigma_\theta|_{Zone\ I} = \sigma_\theta|_{Zone\ II} \tag{56-b}$$

$$at\ r = R_p\ , \qquad \sigma_r|_{Zone\ II} = \sigma_r|_{Elastic} \tag{56-c}$$

$$at\ r = R_p\ , \qquad \sigma_\theta|_{Zone\ II} = \sigma_\theta|_{Elastic} \tag{56-d}$$

$$at\ r = R_p\ , \qquad \sigma_z|_{Zone\ II} = \sigma_z|_{Elastic} \tag{56-e}$$

The closed form solution of Eq. (54) seems to be very difficult therefore; in this paper an appropriate numerical approach is used (see Appendix C). The results for the Eqs. (54), (52) and (31) are expected to be in the following form

$$\sigma_r = a - \frac{b}{r^2} \tag{57}$$

$$\sigma_\theta = a + \frac{b}{r^2} \tag{58}$$

$$\sigma_z = \left(a - \frac{b}{r^2}\right) + \left\{m\sigma_c\left(a - \frac{b}{r^2}\right) + s\sigma_c^2\right\}^{\frac{1}{2}} \tag{59}$$

where a and b are constants.

3.5. Case 5

Fig. 2-d and Fig. 2-e illustrate that case 5 is the same as case 4, where $R_1 = R_0$. Therefore, in case 5, σ_r, σ_θ and σ_z for the plastic zone can be determined from Eqs. (57), (58) and (59), respectively. On the other hand, the elastic stress components are similar to those given by Eqs. (14) to (16), except that the unknown constant C_4^I which should be replaced with the new unknown constant C_4^V.

The four undetermined parameters are: R_p, C_4^V and the two constants result from the solution of Eq. (54). The required boundary conditions can be listed as

$$at\ r = R_0\ , \qquad \sigma_r|_{Plastic} = 0 \tag{60-a}$$

$$at\ r = R_p\ , \qquad \sigma_r|_{Plastic} = \sigma_r|_{Elastic} \tag{60-b}$$

$$at\ r = R_p\ , \qquad \sigma_\theta|_{Plastic} = \sigma_\theta|_{Elastic} \tag{60-c}$$

$$at\ r = R_p\ , \qquad \sigma_z|_{Plastic} = \sigma_z|_{Elastic} \tag{60-d}$$

4. The necessary conditions for occurrence of different cases

Based on different combination of P and P_z, one of the cases 1 to 5 can be occurred. The conditions that P and P_z should satisfy for the occurrence of cases 1-5 are discussed in this section.

Comparison between Fig. 2a and Fig. 2b shows that case 1 is the same as case 2, if $R_1 = R_0$. On the other hand, It is obvious that always $R_1 \geq R_0$. Let P_{z1} be a specific value of P_z, so that at this value, R_1 equals to R_0. Substituting $R_1 = R_0$ in Eq. (24) (For more details, see Appendix D) results in:

$$P_{z1} = 2\mu P + (1-\mu)\sigma_c s^{\frac{1}{2}} \tag{61}$$

Eqs. (25), (26) and (27) illustrate that only m_3 relates to P and P_z. For a constant value of P, the parameter m_3 increases with the increase of P_z. On the other hand, Eq. (24) shows that the value of R_1 increases with the increase of m_3. So, R_1 increases with the increase of P_z. The minimum value of R_1 is R_0, where in this condition, $P_z = P_{z1}$. Therefore, if $P_z \leq P_{z1}$, case 1 occurs and if $P_z \geq P_{z1}$, case 2.

Fig. 2-b, Fig. 2-c and Fig. 2-d show that both of cases 2 and 4 are the same as case 3, if $R_1 = R_p$. On the other hand, It is obvious that always $R_1 \leq R_p$. Let P_{z2} be a specific value of P_z, so that at this value, R_1 equals to R_p. Substituting $R_1 = R_p$ in Eqs. (24) and equating it with Eq. (29) (for more details, see Appendix D) results in:

$$P_{Z2} = 2\mu P + \frac{m_2^2 - \left[m_1 - 2m_1\left[\left(\frac{1}{4} + \frac{P\mathcal{C}^{\ 2}}{C_3}\right)^{\frac{1}{2}} - C_1\right] - 2m_1C_1 - m_2\right]^2}{4m_1} + C_2(1-2\mu) \tag{62}$$

Therefore, the condition of occurrence of case 2 changes to $P_{z1} \leq P_z \leq P_{z2}$; if $P_z = P_{z2}$, case 3 occurs and if $P_z \geq P_{z2}$ case 4.

Let P_{z3} be a specific value of P_z, so that at this value, R_p approaches to infinity. In this condition, the H-B failure criterion of case 4 can be rewritten as

$$P_{z3} = P + \left(mP\sigma_c + s\sigma_c^{\ 2}\right)^{\frac{1}{2}} \tag{63}$$

Finally, the maximum strength of the surrounding rock will be at a value of $P_z = P_{z3}$.

5. Results and Discussions

In this section, the results for the plastic zone radius, the radial, tangential and axial stress components, obtained from the present theory have been compared with those obtained by using M-C failure criterion. The plastic zone radii, based on two different failure criteria, M-C and H-B, have also been compared with the available experimental data.

For all cases, the properties of the rock mass are the same (Table 1). The in situ stress is taken as $P = 30$ MPa and the radius of tunnel, R_0, has been assumed to be 3 meters.

TABLE 1

Properties of the rock sample

σ_c (MPa)	E (GPa)	μ	m	S	C (MPa)	φ (Degree)
80	8.944	0.25	2.012	0.0039	4.21	32.07

The values of P_{z1}, P_{z2} and P_{z3}, obtained here have been compared with the results using the Mohr-Coulomb failure criterion (Zhong Lu et al., 2010) (Table 2).

TABLE 2

The results of P_{z1}, P_{z2} and P_{z3} (MPa) for P = 30 MPa

M-C Criterion (Wang et al., 2009)			H-B Criterion		
P_{z1}	P_{z2}	P_{z3}	P_{z1}	P_{z2}	P_{z3}
26.4	49.5	111.4	18.7	50.1	99.7

5.1. Results for Case 1

It is assumed that $P_z = 15$ MPa, which is less than P_{z1} (for failure criteria). Fig. 3 shows the radial, tangential and axial stress components, obtained from the H-B and M-C criteria. Fig. 3 illustrates that the radial stress, σ_r, obtained from the two theories are very close to each other. In addition, for all stress components, as r increases, the difference between the Mohr-Coulomb and Hoek-Brown results decreases. The plastic zone radii, obtained from M-C and H-B failure criteria, are 4.55 and 4.65 meters, respectively.

Eq. (20) illustrates that plastic zone radius, R_p, only relates to P, not to P_z. Fig. 4 shows the values of R_p, with respect to P, for case 1 using M-C and H-B failure criteria. It is assumed that the value of P_z is equal to 15MPa. The results show that the plastic zone radii predicted by H-B criterion is a few more than those of M-C criterion.

5.2. Results for Case 2

In this case, $P_z = 40$ MPa and $P_{z1} \leq P_z \leq P_{z2}$, (for both failure criteria). Fig. 5 shows the radial, tangential and axial stress components, obtained by using the H-B and M-C criteria. In section 3.2, it was mentioned that in plastic zones I and II, the radial and tangential stress components, σ_r and σ_θ, can be obtained from Eqs. (8), (11) respectively. In addition, the axial stress component, σ_z, in the plastic zone I is equal to σ_θ and in the plastic zone II can be determined

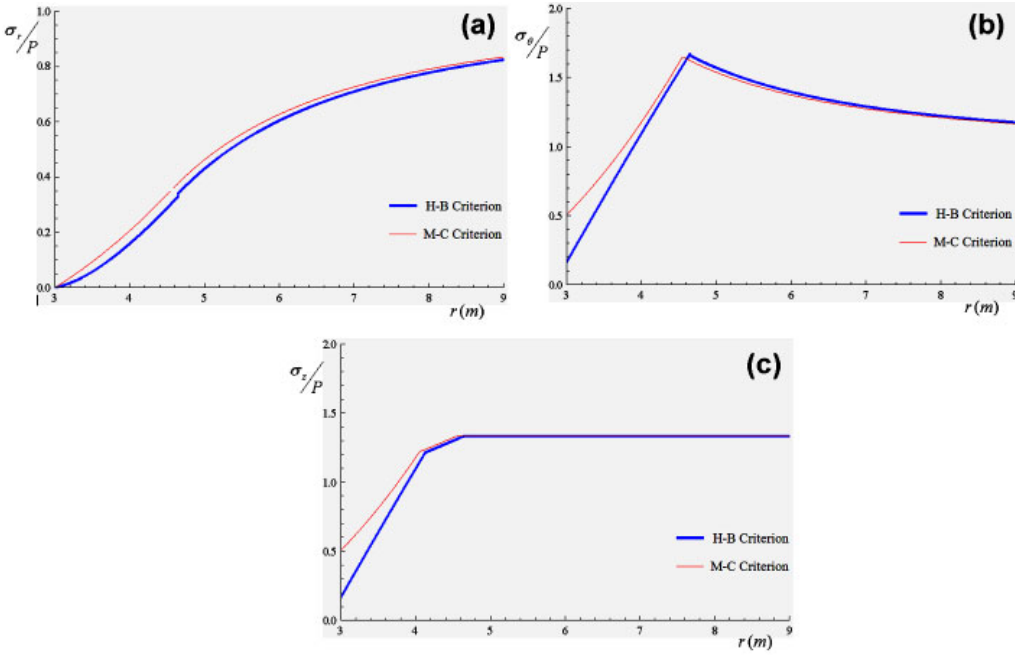

Fig. 3. Distribution of stress components for case 1, P = 30 MPa, P_z = 15 MPa, a) Radial stress, b) Tangential stress, c) Axial stress

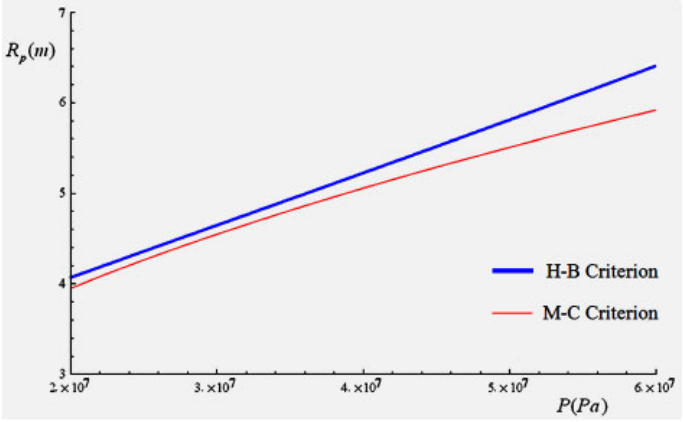

Fig. 4. Variation of R_p with constant P_z(P_z = 15 MPa) and various P

from Eq. (13). In other words, in the plastic zone, σ_r and σ_θ are formulated by one function while σ_z is formulated by two functions. The radii of the plastic zone I, obtained from M-C and H-B failure criteria, are 4.05 and 4.13 meters, respectively, while the radii of the plastic zone II are the same as those of case 1.

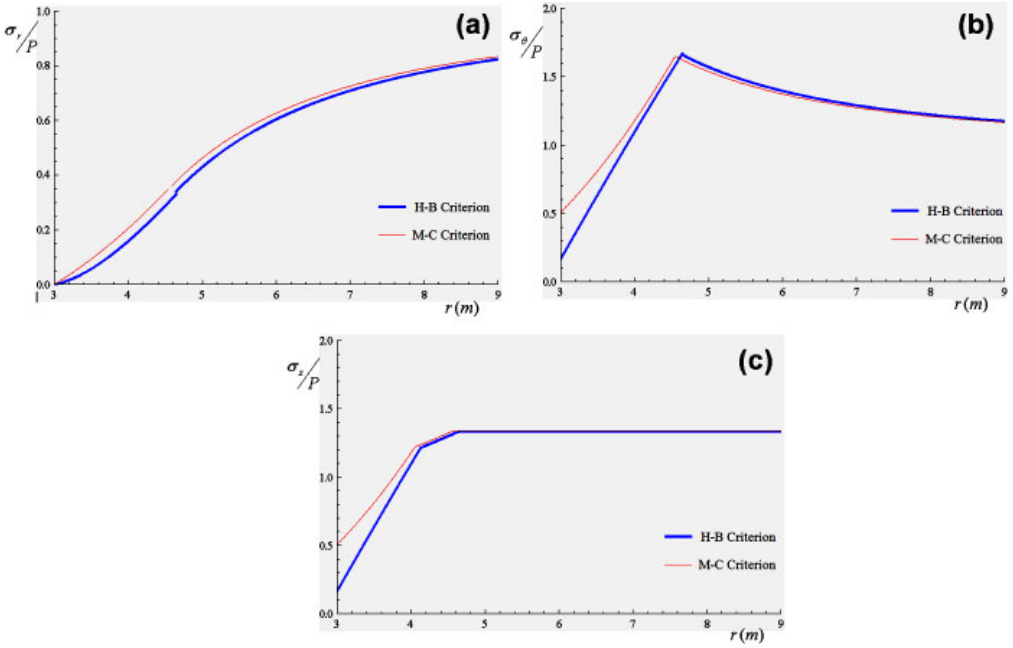

Fig. 5. Distribution of stress components for case 2, P = 30 MPa, P_z = 40 MPa,
a) Radial stress, b) Tangential stress, c) Axial stress

Figs. 6 and 7 show the obtained radius of the plastic zone I, R_1, for case 2 using the M-C and H-B failure criteria, respectively.

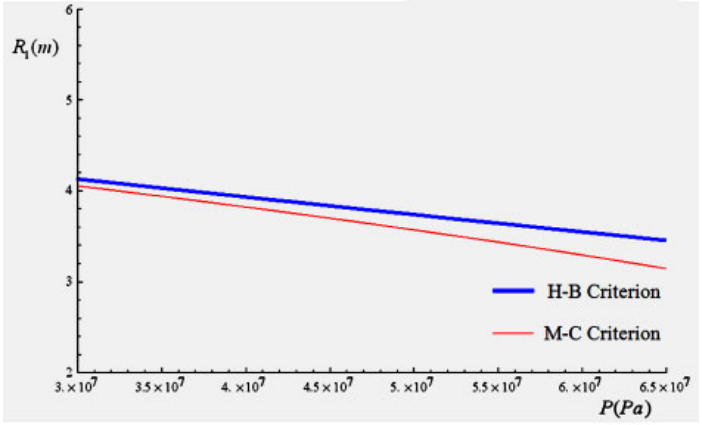

Fig. 6. Variation of R_1 for a constant P_z(P_z = 40 MPa) and various values of P

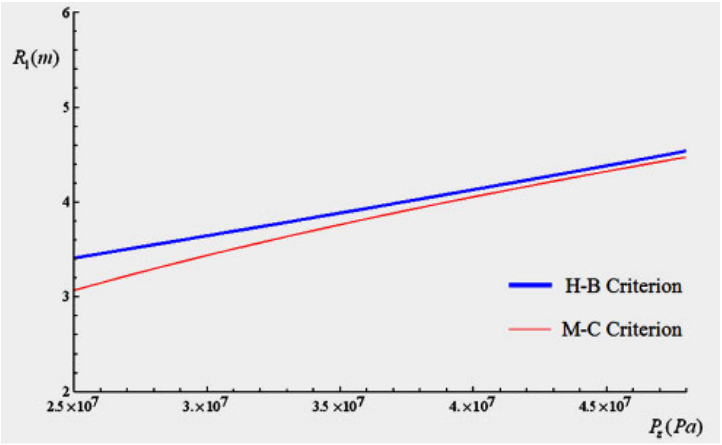

Fig. 7. Variation of R_1 for constant P (P = 30 MPa) and various values of P_z

5.3. Results of Case 3

It was mentioned (in sections 3.3 and 4) that in case 3, $P_z = P_{z2}$ and $R_1 = R_p$. In other words, replacing P_z with P_{z2} leads to $R_1 = R_p$.

In this case, the stress components can be obtained by replacing P_z (in case 2) with P_{z2}. Fig. 8 shows the axial stress component, σ_z, based on H-B failure criterion (it has been obtained from case 2 by replacing P_z with P_{z2}). Comparing Fig. 8 with Fig. 5-c illustrates that Fig. 8 is the same as Fig 5-c, if R_1 converges to R_p.

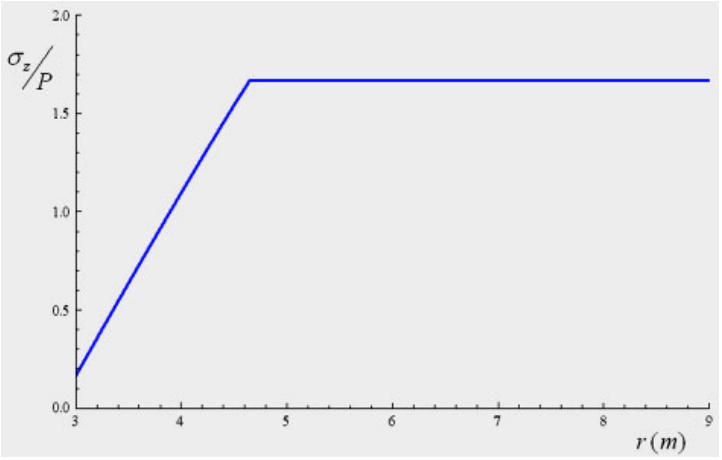

Fig. 8. Variation of σ_z/P with respect to r for case 3, P = 30 MPa, $P_z = P_{z2}$

5.4. Results of Case 4

In this case, P_z = 70 MPa and $P_{z2} \leq P_z \leq P_{z3}$, (obtained from both failure criteria). The radial, tangential and axial stress components, obtained from H-B and M-C criteria, have been shown in Fig. 9. In this case (unlike case 2), all of the stress components, σ_r, σ_θ and σ_z have two functions in the plastic zone.

In case 4, the plastic zone radii, R_1 and R_p are calculated numerically.

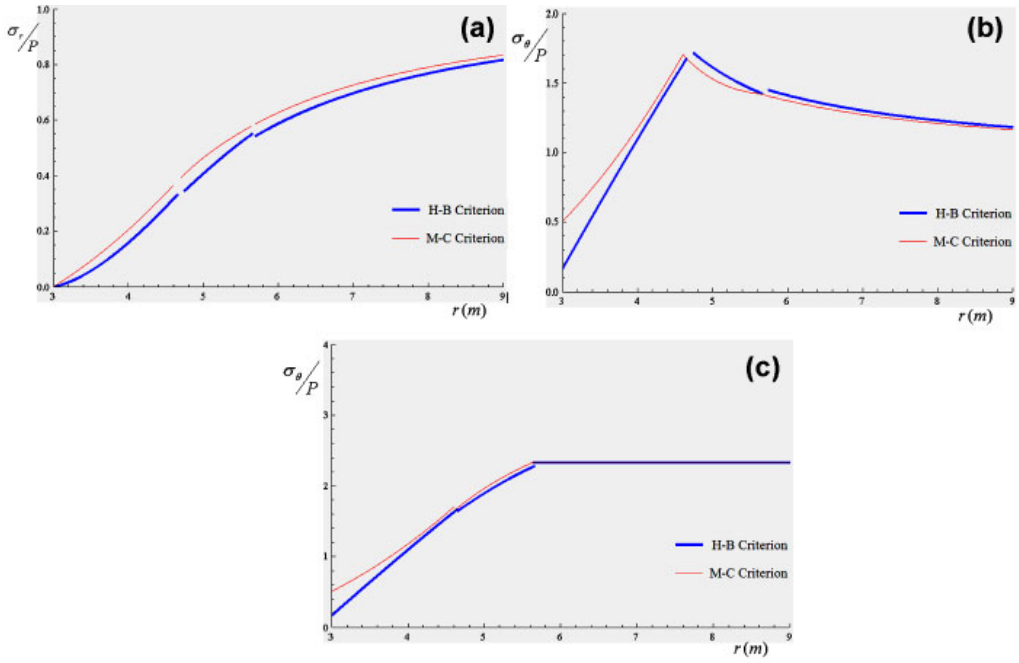

Fig. 9. Distribution of stress components for case 4, P = 30 MPa, P_z = 70 MPa,
a) Radial stress, b) Tangential stress, c) Axial stress

5.5. Comparison of the theoretical plastic zone radius with the experimental data

The plastic zone radius, obtained from M-C and H-B failure criteria, have been compared with the plastic zone radius obtained with experimental data obtained by observational methods in Emamzade Hashem tunnel of Iran (*Technical Deputy*..., 2002). The properties of the rock mass in the different sections of tunnel are shown in Table 3. The tunnel radius, R_0, is about 5.8 m and the in situ stress, P is equal to 10 MPa.

TABLE 3

Properties of rock mass in the different sections of Emamzade Hashem tunnel (*Technical Deputy*..., 2002)

Sample No.	σ_c (MPa)	E (GPa)	μ	m	S	C (MPa)	φ (Degree)	R_p (m)
1	40	1.5	0.25	0.606	0.0017	0.825	29.2	13.9
2	40	1.5	0.26	0.800	0.003	0.735	35.3	11.3
3	38	1.5	0.27	0.523	0.002	0.683	29.94	13.1
4	40	1.5	0.26	0.736	0.0026	0.726	34.27	11.7
5	41	1.5	0.27	0.860	0.0034	0.796	35.59	11.5
6	41	1.5	0.25	1.065	0.0042	0.865	37.16	11.2
7	42	1.5	0.24	1.443	0.0052	0.982	39.47	11.0
8	41	1.5	0.24	1.209	0.0047	0.936	37.61	11.3

Fig. 10 compares the theoretical results, based on two different failure criteria, and the results obtained from the experimental data. Except the sample number 3, in all other samples the experimental results are greater than those of obtained by M-C and H-B criteria. Fig. 10 shows that the Hoek-Brown failure criterion can predict the plastic zone radius with slightly better accuracy compared to the Mohr-Coulomb failure criterion. Implementing the least squares error method, it can be concluded that the error in R_p using H-B criterion is about 14.3%, while that of using M-C Criterion is about 16.1%.

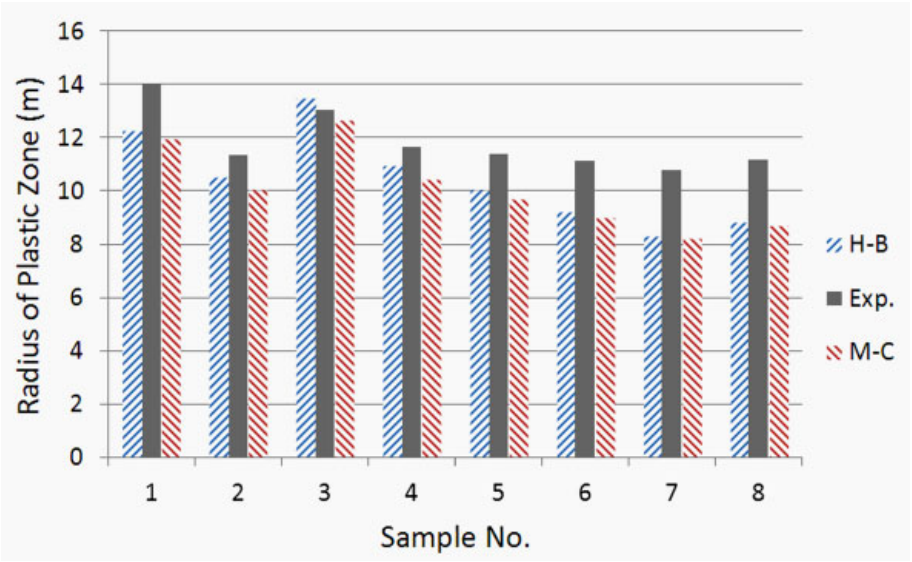

Fig. 10. Comparing the plastic zone radius (using M-C and H-B failure criteria, and experimental data)

6. Conclusion

In this study, using the non-linear Hoek-Brown failure criterion, a new analytical method is proposed for estimating the stress components and plastic zone radius around a circular tunnel subjected to a plane hydrostatic and an axial in situ stresses. The radial stress, σ_r, obtained based on M-C and H-B criteria are in good agreement with each other, but the other stress components, σ_θ and σ_z, (obtained also by using M-C and H-B criteria) have a meaningful difference in the vicinity of the tunnel boundary. For all the stress components, with the increasing in r, the difference between the M-C and H-B results decreases. In the plastic zone, all of stress components, σ_r, σ_θ and σ_z, determined based on M-C failure criterion are more than those of determined based on H-B failure criterion. Considering a non-linear failure criterion (Hoek-Brown), affects slightly on the determined plastic zone radius, in such way as that the plastic zone radii predicted by H-B criterion are a little more than those predicted by using the M-C criterion. The difference between the corresponding plastic radii obtained by using Mohr-Coulomb and Hoek-Brown failure criteria increases with the increasing in P/P_z ratio. Both of M-C and H-B failure criteria underestimate the plastic zone radius. However, the error in R_p using H-B criterion is a little less than that obtained by using the M-C criterion.

References

Borecki M., Chudek M., 1972. *Rock mechanics*. Ślaśk Publishers, Katowice.

Brady E.T., Brown B.H.G., 2004. *Rock mechanics for underground mining*. Springer, 3rd Ed.

Brown E.T., Bray J.W., Ladanyi B., Hoek E., 1983. *Ground response curves for rock tunnels*. ASCE J. Geotech. Eng., 109, 15-39.

Carranza-Torres C., 2004. *Elasto-plastic solution of tunnel problem using the generalized form of the Hoek-Brown failure criterion*, Int. J. Rock Mech. Min. Sci., 41(3), 480-1.

Carranza-Torres C., Fairhurst C., 1999. *The elasto-plastic response of underground excavations in rock masses that satisfy the Hoek-Brown failure criterion*, Int J Rock Mech. Min. Sci., 36, 777-809.

Chudek M., 1986. *Roof bolting. Part 1. Supports for tunnel headings and caverns*. Śląsk, Katowice.

Detournay E., 1986. *Elastoplastic model of a deep tunnel for a rock with variable dilatancy*. Rock Mech. Rock Eng., 19, 99-108.

Duży S., 2007. *Reliability analysis of support structure and stability of tunnel headings in collieries, taking into account the uncertainty of information*. Journals of Silesian Polytechnics, no 1750.

Guan Z., Jiang Y., Tanabasi Y., 2007. *Ground reaction analyses in conventional tunneling excavation*. Tunnel Undergr. Space Technol., 22, 230-7.

Hoek E., Brown E.T., 1980. *Underground excavation in rock*. London, I.M.M.

Keryszig E., 2006. *Advanced engineering mathematics*. John Wiley, 10th Ed.

Kłeczek Z., 1994. *Mining geomechanics*. Śląskie Wydawnictwo Techniczne, Katowice.

Lee Y.K., Pietruszczak S., 2008. *A new numerical procedure for elasto- plastic analysis of a circular opening excavated in a strain- softening rock mass*, Tunnelling and Underground Space Technology.

Majcherczyk T., 1995. *Influence of roof bolts on the rock mass parameters*. Archives of Mining Sciences 4.

Park K.H., Kim Y.J., 2006. *Analytical solution for a circular opening in an elastic-brittle-plastic rock*, Int. J. Rock Mech. Min. Sci., 43, 616-22.

Popov E.P., 1990. *Strength of Materials*. 2nd Ed., D. Van Nostrand Co.

Reed M.B., 1986. *Stresses and displacements around a cylindrical cavity in soft rock*. Inst. Math. Anal. J. Appl. Math., 36, 223-45.

Saad M., 2009. *Elasticity, Theory, Application and Numerics*. Academic Press.

Salustowicz A., 1965. *Zarys mechniki górotworu*. Wyd. Slask. Katowice.

Sharan S.K., 2003. *Elastic-brittle-plastic analysis of circular openings in Hoek–Brown media*, Int. J. Rock Mech. Min. Sci., 40, 817-24.

Sharan S.K., 2005. *Exact and approximate solutions for displacements around circular openings in elastic-brittle-plastic Hoek-Brown rock*, Int. J. Rock Mech. Min. Sci., 42, 542-9.

Sharan S.K., 2008. *Analytical solutions for stresses and displacements around a circular opening in a generalized Hoek-Brown rock*, Int. J. Rock Mech. Min. Sci., 45, 78-85.

Tajduś A., Wichur A., 2009. *Underground structures in Poland- current expertise and practice (commemorating the 90th anniversary of AGH-UST)*. Mining Journal 5-6.

Technical Deputy of Hara Institute, The reports collection on the 1st variant of Emam Zade Hashem tunnel (IRAN), 2002.

Timoshenko S., 2010. *Strength of Materials*, 7th Ed, Krieger.

Wang Y., 1996. *Ground response of circular tunnel in poorly consolidated rock*. J. Geotech. Eng., 122, 703-8.

Wang S., Yin X., Tang H., Ge X., 2009. *A new approach for analyzing circular tunnel in strain-softening rock masses*, Int. J. Rock Mech. Min. Sci., 43, 102-112.

Wichur A., 2009. *Design of roof bolts in underground excavations*. Górnictwo i Geoinżynieria (Mining and Geoengineering) 3/1.

Zhong Lu A., Xu G., Sun F., Sun W., 2010. *Elasto-plastic analysis of a circular tunnel including the effect of the axial in situ stress*. Int. J. Rock Mech. Min. Sci., 47(1), 50-59.

Received: 15 November 2011

APPENDIX A

Solving Eqs. (18) and (19) in order to find R_p and C_4^I;

$$C_3(LnR_p + C_1)^2 + C_2 = P - C_4^I / R_p^2 \tag{A-1}$$

$$C_3(LnR_p + C_1)^2 + 2C_3(LnR_p + C_1) + C_2 = P + C_4^I / R_P^2 \tag{A-2}$$

Adding Eqs. (A-1) and (A-2) gives:

$$2C_3(LnR_p + C_1)^2 + 2C_3(LnR_p + C_1) + 2C_2 = 2P \tag{A-3}$$

Assuming $Ln\ R_p + C_1 = t$, Eq. (A-3) can be convert to Eq. (A-4):

$$t^2 + t - \frac{P - C_2}{C_3} = 0 \tag{A-4}$$

Solving Eq. (A-4) for t results in:

$$t = -\frac{1}{2} \pm \sqrt{\frac{1}{4} + \frac{P - C_2}{C_3}} \tag{A-5}$$

It is obvious that:

$$Ln R_p + C_1 = Ln R_p + \frac{2s^{1/2}}{m} - Ln R_0 > 0 \tag{A-6}$$

So:

$$t = Ln R_p + C_1 = -\frac{1}{2} + \sqrt{\frac{1}{4} + \frac{P - C_2}{C_3}} \tag{A-7}$$

Solving Eq. (A-7) for R_p leads to:

$$R_p = \exp\left[\frac{1}{2} + \sqrt{\frac{1}{4} + \frac{P - C_2}{C_3}} + C_1\right] \tag{A-8}$$

Substituting Eq. (A-8) into Eq. (A-1), C_4^I can be obtained as:

$$C_4^I = R_p^2 \left[P - C_3 (Ln R_p + C_1)^2 + C_2\right] \tag{A-9}$$

APPENDIX B

Solving Eq. (23) for the radius of the plastic zone I, R_1;

$$\begin{aligned} &C_3(LnR_1 + C_1)^2 + 2C_3(LnR_1 + C_1) + C_2 = \\ &\quad = 2\mu\left[C_3(LnR_1 + C_1)^2 + C_3(LnR_1 + C_1) + C_2\right] + P_z - 2\mu P \end{aligned} \tag{B-1}$$

Assuming $Ln\, R_1 + C_1 = t$, Eq. (B-1) converts to:

$$C_3 t^2 + 2C_3 t + C_2 = 2\mu[C_3 t^2 + C_3 t + C_2] + P_z - 2\mu P \tag{B-2}$$

Eq. (B-2) can be written as:

$$m_1 t^2 + m_2 t + m_3 = 0 \tag{B-3}$$

where:

$$m_1 = 2C_3\mu - C_3 \tag{B-4}$$

$$m_2 = 2C_3\mu - 2C_3 \tag{B-5}$$

$$m_3 = 2C_2\mu + P_z - 2\mu P - C_2 \tag{B-6}$$

Solving Eq. (B-3) for t gives:

$$t = \frac{-m_2 \pm \sqrt{m_2^2 - 4m_1 m_3}}{2m_1} \tag{B-7}$$

Since $t \geq 0$ and $m_1 \leq 0$ (see Eq. (B-4)):

$$t = \frac{-m_2 - \sqrt{m_2^2 - 4m_1 m_3}}{2m_1} \tag{B-8}$$

So:

$$R_1 = \exp\left[\frac{-m_2 - \left(m_2^2 - 4m_1 m_3\right)^{\frac{1}{2}}}{2m_1} - C_1\right] \tag{B-9}$$

APPENDIX C

Solving Eq. (54) with considering boundary conditions (Eq. (56));

$$r^2 \frac{d^2\sigma_r}{dr^2} + 3r\frac{d\sigma_r}{dr} = g(\sigma_r) \tag{C-1}$$

In order to solve Eq. (C-1), the Euler's method is used (Keryszig, 2006). Between R_1 and R_p, several points are defined (in this work 18 points were defined). The initial guesses for R_1 and R_p are considered. From Eqs. (56-a) and (56-b) the values of σ_r and σ_θ in $r = R_1$ are determined. Substituting σ_r and σ_θ for $r = R_1$ into Eq. (52), $\frac{d\sigma_r}{dr}$ in $r = R_1$ is obtained. By considering σ_r and $\frac{d\sigma_r}{dr}$ in $r = R_1$, the value of σ_r for the other points is calculated. Substituting the value of σ_r, obtained for the last point (at $r = R_p$) into Eqs. (31) and (52), gives σ_θ and σ_z. Substituting the obtained values of σ_r, σ_θ and σ_z for $r = R_p$ into Eqs. (56-c) and (56-d), C_4^{IV} and the new value of R_p are calculated. On the other hand, the new value of R_p can be calculated by substituting the obtained values of σ_r, σ_θ and σ_z for $r = R_p$ into Eq. (56-e). If the two new values of R_p are equal together, the initial guesses for R_1 and R_p are correct. Else, the new initial guesses must be considered and the approach repeated.

APPENDIX D

Determination of P_{z1}, P_{z2} and P_{z3};

Calculation of P_{z1};
Replacing R_1 in Eq. (24) with R_0 gives:

$$\exp\left[\frac{-m_2 - \left(m_2^2 - 4m_1 m_3\right)^{\frac{1}{2}}}{2m_1} - C_1\right] = R_0 \tag{D-1}$$

So:

$$\frac{-m_2-\left(m_2^2-4m_1m_3\right)^{\frac{1}{2}}}{2m_1}-C_1=LnR_0 \tag{D-2}$$

Rewriting Eq. (D-2) gives:

$$\left(m_2^2-4m_1m_3\right)^{\frac{1}{2}}=-2m_1\left(LnR_0+C_1\right)-m_2 \tag{D-3}$$

Or:

$$\left(m_2^2-4m_1m_3\right)=\left[-2m_1\left(LnR_0+C_1\right)-m_2\right]^2 \tag{D-4}$$

Eq. (D-4) can be simplified as:

$$\left(m_2^2-4m_1m_3\right)=4m_1^2\left(LnR_0+C_1\right)^2+m_2^2+4m_1m_2\left(LnR_0+C_1\right) \tag{D-5}$$

Solving Eq. (D-5) for m_3 results in:

$$m_3=-m_1\left(LnR_0+C_1\right)^2-m_2\left(LnR_0+C_1\right) \tag{D-6}$$

Combination Eqs. (D-6) and (27) gives:

$$-m_1\left(LnR_0+C_1\right)^2-m_2\left(LnR_0+C_1\right)=2C_2\mu+P_{z1}-2\mu P-C_2$$

Which can be rearrenged as:

$$P_{z1}=2\mu P+C_2(1-2\mu)-\left(LnR_0+C_1\right)\left[m_1\left(LnR_0+C_1\right)+m_2\right] \tag{D-7}$$

Substituting C_1, C_2, m_1 and m_2 from Eqs. (7), (9), (25) and (26), respectively leads to:

$$P_{z1}=2\mu P+(1-\mu)\sigma_c s^{\frac{1}{2}} \tag{D-8}$$

Calculation of P_{z2};
Substituting R_1 and R_p from Eqs. (24) and (29), respectively gives:

$$\exp\left[\frac{-m_2-\left(m_2^2-4m_1m_3\right)^{\frac{1}{2}}}{2m_1}-C_1\right]=\exp\left[-\frac{1}{2}+\sqrt{\frac{1}{4}+\frac{P-C_2}{C_3}}-C_1\right] \tag{D-9}$$

Or:

$$\frac{-m_2-\left(m_2^2-4m_1m_3\right)^{\frac{1}{2}}}{2m_1}-C_1=-\frac{1}{2}+\sqrt{\frac{1}{4}+\frac{P-C_2}{C_3}}-C_1 \tag{D-10}$$

Eq. (D-10) can be rewritten as:

$$\left(m_2^2-4m_1m_3\right)^{\frac{1}{2}}=m_1-2m_1\left[\left(\frac{1}{4}+\frac{P-C_2}{C_3}\right)^{\frac{1}{2}}-C_1\right]-2m_1C_1-m_2 \tag{D-11}$$

Or:

$$m_2^2-4m_1m_3=\left[m_1-2m_1\left[\left(\frac{1}{4}+\frac{P-C_2}{C_3}\right)^{\frac{1}{2}}-C_1\right]-2m_1C_1-m_2\right]^2 \tag{D-12}$$

Solving Eq. (D-12) for m_3 results in:

$$m_3=\frac{m_2^2-\left[m_1-2m_1\left[\left(\frac{1}{4}+\frac{P-C_2}{C_3}\right)^{\frac{1}{2}}-C_1\right]-2m_1C_1-m_2\right]^2}{4m_1'} \tag{D-13}$$

Combination Eqs. (D-13) and (27) gives:

$$\frac{m_2^2-\left[m_1-2m_1\left[\left(\frac{1}{4}+\frac{P-C_2}{C_3}\right)^{\frac{1}{2}}-C_1\right]-2m_1C_1-m_2\right]^2}{4m_1'}=2C_2\mu+P_{z2}-2\mu P-C_2 \tag{D-14}$$

Rewriting Eq. (D-14) results:

$$P_{z2}=2\mu P+\frac{m_2^2-\left[m_1-2m_1\left[\left(\frac{1}{4}+\frac{P-C_2}{C_3}\right)^{\frac{1}{2}}-C_1\right]-2m_1C_1-m_2\right]^2}{4m_1}+C_2(1-2\mu) \tag{D-15}$$